

Deposition and Characterization of ZnS/Si Heterojunctions Produced by Vacuum Evaporation

(NASA-TM-101359) DEPOSITION AND
CHARACTERIZATION OF ZnS/Si HETEROJUNCTIONS
PRODUCED BY VACUUM EVAPORATION (NASA) 18 p
CSCL 09C

N89-11129

Unclassified
G3/33 0170247

Geoffrey A. Landis
Lewis Research Center
Cleveland, Ohio

and

Joseph J. Loferski and Roland Beaulieu
Brown University
Providence, Rhode Island

Prepared for the
Fifth North Coast American Vacuum Society Symposium
Cleveland, Ohio, June 2, 1988





Deposition and Characterization of ZnS/Si Heterojunctions Produced by Vacuum Evaporation

Geoffrey A. Landis*,
NASA Lewis Research Center,
Cleveland, OH 44135

Joseph J. Loferski and Roland Beaulieu
Brown University,
Providence, RI 02912

Abstract

Isotype heterojunctions of ZnS (lattice constant 5.41 Å) were grown on silicon (lattice constant 5.43 Å) p-n junctions to form a minority-carrier mirror. The deposition process was vacuum evaporation from a ZnS powder source onto a heated (450° C) substrate. Both planar (100) and textured (111) surfaces were used. A reduction of the minority-carrier recombination at the surface was seen from increased short-wavelength quantum response and increased illuminated open-circuit voltage. The minority carrier diffusion length was not degraded by the process.

INTRODUCTION

Achieved open circuit voltage (V_{oc}) of current silicon solar cells falls well below theoretically predicted values of 700 to 800 mV. The voltage is controlled by carrier recombination in the base, the emitter, and the front and back surfaces. The next generation of high efficiency cells will require very low surface recombination at both front and back surfaces.

One approach to reducing surface recombination is growth of an epitaxial heterojunction "window" of a higher bandgap material on the surface.

*National Research Council—NASA Research Associate.

The material for a window layer for use on silicon must satisfy the following criteria:

- (1) Transparent across the solar spectrum
- (2) Low interface recombination.
- (3) Low resistance contact.

Candidate semiconductors which meet many or all of the criteria include ZnS, CdS, ZnSe, AlP, GaP, and indium-tin oxide ("ITO")

Transparency requires a bandgap of at least 3 eV in order that few photons of the solar spectrum are absorbed by the window. Low density of interface states can be aided by growth of the window layer in epitaxial form, rather than polycrystalline. In epitaxial growth, the crystal structure of the substrate is continued by the deposited layer. Epitaxial growth on silicon requires a semiconductor with fcc structure and a lattice constant equal to or close to 5.431 angstrom. Of the semiconductor materials available, ZnS, with a bandgap of 3.6 eV and a lattice constant 5.406 angstrom, appears to best meet the criteria for a window layer.

STATEMENT OF PROBLEM

For the best currently made single-crystal solar cells, short circuit current is very close to ideal. While some improvements are still possible, major increases are not likely. Open circuit voltage, V_{oc} , on the other hand, is considerably lower than theoretical studies predict should be achievable. This suggests that V_{oc} is the most promising target for further improvements in silicon solar cell efficiencies. Increasing V_{oc} requires decreasing the reverse saturation current, I_o .

The saturation current arises from minority carriers which are injected across the junction to recombine either in the bulk, in the emitter, or on one of the surfaces. Thus, the technical problem can be broadly identified as that of finding a means of lowering the recombination rate of minority carriers.

For example, in conventional thick, 10 $\Omega\text{-cm}$ base cells, base recombination is the major component of the dark current. Thus, open circuit voltage can be significantly improved only by changes in the base: either making it thinner (thus decreasing the volume for carriers to recombine in), increasing the minority carrier lifetime (thus decreasing the

recombination rate), or increasing the doping (thus decreasing the injection of carriers across the junction).

If the cell is made thinner, rear surface recombination can become the dominant component of the dark current. This can be decreased by reducing the back surface recombination velocity, for example, by forming a back surface field (BSF) to keep minority carriers from approaching the back surface. This is one example of a minority carrier mirror (MCM).

On actual cells, base resistivity can be reduced to about 0.15 to 0.30 $\Omega\text{-cm}$. Increasing the base doping beyond this point actually decreases V_{oc} , because of a rapid decrease in material quality at higher doping levels, as well as a decrease in minority carrier lifetime due to increased recombination centers and the onset of heavy doping effects, such as Auger recombination.

Doping of about 0.3 $\Omega\text{-cm}$ is used on the highest efficiency cells currently made. At these base doping levels, the recombination current tends to be dominated by the emitter and front surface. Conventional solar cells use extremely high emitter doping, usually as high as 10^{20} ions/cm³ or higher. This has the effect of completely shielding the front surface from the minority carriers, but has the disadvantage of being so highly doped that the emitter is well into the range of heavy doping, and thus, emitter dark current begins to dominate the recombination.

The main approach to reducing emitter dark current is to lower the emitter doping. This results in an emitter which is "narrow", or "transparent" to minority carriers; that is, minority carriers can traverse completely through the emitter without recombining, and arrive at the front surface. Low doping emitters are thus only practical if the front surface has a low recombination velocity. This is often referred to as surface passivation. Thus, the specific technical problem can be seen to be finding an effective method of surface passivation of silicon solar cells which does not otherwise affect the performance of the cell [1].

The best solar cells currently made use a thin thermal oxide layer to passivate the surface. The interface between silicon and silicon dioxide is a low, but not zero, recombination velocity surface. This approach is often recommended as the route to future extremely high efficiency cells. However, there is a limit to the amount of surface passivation which can be achieved by use of an oxide surface. Silicon dioxide is an insulator, thus, it

cannot be present on the surface under the metal contacts. Since ohmic contacts have nearly infinite surface recombination velocity, this unpassivated area puts a limit on the amount of V_{oc} improvement which can be achieved by the use of oxide. The best silicon cells reduce, but do not eliminate, this recombination by decreasing the contact area of the cell. This approach is often recommended as the route to future extremely high efficiency cells [2].

A suggested "fix" to this problem would be to use a heavily doped region under the contact fingers, to serve as a field region to repel minority carriers from the ohmic contact. However, there are limits to the degree in which this can be achieved before heavy doping effects again limit V_{oc} .

The optimum surface layer would be "transparent" to majority carrier current flow but reflect minority carriers completely, ie. a minority carrier mirror. This can be achieved by use of a heterojunction "window" of a second semiconductor with a band gap wider than the base (silicon).

Use of heterojunction window layers to confine minority carriers is common in III-V technology. For example, in a double-heterostructure injection laser, the active layer, usually gallium arsenide, is sandwiched between two layers of a wider bandgap semiconductor, gallium aluminum arsenide, in order to confine the injected carriers to the laser region. The same technology is used for high efficiency gallium arsenide solar cells, where a surface layer of gallium aluminum arsenide serves as a zero surface recombination velocity interface, and in amorphous silicon (a-Si) solar cells, where a window layer of amorphous silicon carbide is typically used. The window layer approach is common on III-V semiconductors such as gallium arsenide because there exist naturally lattice-matched systems within the III-V group, such as the GaAs-AlAs ternary system. Within this ternary system, compounds can be grown with a wide range of bandgaps at the same lattice constant. Use of this approach on silicon is not commonly done. Prior to this work and the companion work using MO-CVD done at Spire [3], we know of no previous use of electrically active, lattice matched wide-bandgap heterojunctions on silicon. This is probably because of the much more restricted choice of materials with a match to the smaller lattice constant of silicon, 5.431 Ångstroms.

For a surface passivation layer on the front surface of a solar cell, it is important that the layer not absorb light in the wavelength band used by the

cell. (For passivation of the rear surface, this is not critical.) This makes a much more restricted choice of material for the front surface passivation than for the rear surface passivation. Semiconductors are nearly transparent for all photons of energy less than their bandgap, and absorbing for photons of energy greater than the bandgap. All of the photons of energy greater than the bandgap of silicon, 1.08 eV, out to the cut-off of the solar spectrum [4] are potentially usable. In order that the window layer not greatly decrease the short circuit current, the bandgap should be larger than 2.5 eV, and preferably at least 3 eV.

Finally, for contact to a n-type surface, the electron affinity of the deposited layer should be matched (or nearly matched) to that of the substrate material, in order to avoid a discontinuity ("spike") in the conduction band which would provide a barrier to current flow [5].

Figure 1 shows the band diagram of an ideal heterojunction minority carrier mirror.

Table 1 lists the bandgaps, lattice constants, and electron affinity of the III-V and II-VI semiconductors [6]. Each of these has a form with fcc crystal symmetry (matching that of silicon). For silicon, the bandgap is 1.1 eV, the electron affinity 4.01 eV, and the lattice constant 5.431 angstrom.

We can see from this list that only one semiconductor, ZnS, has a bandgap over 3 eV. ZnSe, CdS, AlP, ZnTe, GaP, and AlAs, with bandgaps 2.2 to 2.6 eV, are also possible choices.

If the lattice constant is nearly the same as that of silicon, epitaxial growth may be possible. This may result in lower interface state density. Of the semiconductors listed, ZnS, GaP, and AlP have close enough lattice constant matches to that of Silicon to allow high quality epitaxy. These three semiconductors are thus the most likely candidates.

ZnS (Zinc Sulfide) has a lattice constant nearly matching silicon, and has a bandgap over 3 eV and an electron affinity nearly matched to that of silicon, and thus is the best candidate for a heterojunction passivation layer on n-type silicon.

Table 1: Bandgap, Lattice Constant, and Electron Affinity of III-V and II-VI Semiconductors

Material	Bandgap (eV)	Lattice Constant (Å)	Electron Affinity (eV)
III-V			
AlP	2.4	5.45	-
AlAs	2.2	5.65	-
AlSb	1.6	6.15	3.65
GaP	2.3	5.45	4.3
GaAs	1.4	5.65	4.07
GaSb	0.72	6.10	4.06
InP	1.33	5.85	4.38
InAs	0.34	6.05	4.9
InSb	0.18	6.46	4.59
II-VI			
ZnS	3.6	5.41	3.9
ZnSe	2.6	5.67	4.09
ZnTe	2.3	6.10	3.5
CdS	2.4	5.83	4.5
CdSe	1.8	6.06	4.95
CdTe	1.5	6.47	4.28
HgS	2.0	5.86	-
HgSe	0.6	6.07	-
HgTe	-0.02	6.43	-

APPROACH

Because of the above considerations, we proposed a thin heteroepitaxial wide-bandgap layer on the surface of a silicon solar cell as a promising approach to making a low recombination conductive surface, with ZnS the most promising candidate for wide-bandgap semiconductor.

Undoped ZnS has very high resistivity (~70000 Ω-cm). Resistivity as low as 0.64 Ω-cm has been obtained in thin films by Olsen [7] and others, and 1-10 Ω-cm in bulk crystals. ZnS can either be doped by an excess of Zn, or by use of substitutional dopants such as Al or In [7,8]. Electron mobility is

up to about 750 cm²/v-sec; hole mobility considerably lower, about 10 cm²/v-sec. ZnS can only be made n-type. This limits its use as a passivating surface layer to n-type silicon. Fortunately, the electron affinity very nearly matches that of silicon, with a difference of only 0.1 eV, so a n-n heterojunction should have little barrier to majority carriers.

The index of refraction of ZnS ranges from 2.41 at 0.5 microns to 2.29 at 1.1 microns. These indices, along with its high transparency, make it nearly ideal as an antireflective coating.

ZnS has both a cubic (zincblende) and a hexagonal (wurtzite) modification. Above about 1050° C, the hexagonal form is the most stable, while the cubic form is thermodynamically preferred below this temperature. Both modifications are stable at room temperature. The cubic form, which is what we want, will be the modification produced as long as the growth temperature is low compared to 1050° C.

THEORY

The minority carrier recombination at a surface or interface can be usefully approximated by the surface-recombination velocity approximation, where the total number N of excess carriers recombining (per unit area) is linearly related to the excess carrier density (per cubic volume) at the surface by a proportionality constant S. The units of S are thus cm/second, or velocity.

Consider a perfect heterojunction with no interface states and no band bending. The effective interface recombination velocity ("S") at the high-low junction is the fraction of excess carriers which cross the junction, times the rate at which they move into the wide bandgap material to recombine [9]. For a barrier of ΔE_g equal to the difference in bandgaps, the fraction of carriers is simply the number with enough thermal energy to cross the interface, $\exp(-\Delta E_g/kT)$. The effective recombination velocity thus exponentially decreases with the difference in bandgaps. For a heterojunction material with bandgap substantially wider than the substrate, S will be very close to zero.

In actual materials there will be interface states, and the recombination velocity will depend on the density of interface states, the cross section, energy levels, etc. [10]. In the worst case, there will be surface states due to

dangling bonds at the interface caused by mismatch of the lattice constants. For the ZnS/Si heterojunction, the lattice constant mismatch is about 0.39%. This results in a surface state density of about $10^{13}/\text{cm}^2$ if it is assumed that the mismatch is entirely taken up in broken bonds at the interface. If these interface states are in midgap, and have a high capture cross section, then the recombination rate at the interface may be high. However, for a sufficiently thin layer (thinner than $\sim 1000\text{\AA}$), the growth should be a strained, pseudomorphic, layer, with no interfacial dislocations.

ZnS DEPOSITION ON Si

Vacuum Evaporation

Figure 2 shows a schematic of the deposition region of the evaporation system [11]. Evaporation is from a single source.

In order to make epitaxial growth possible, the deposition must be on a substrate held at an elevated temperature. A main factor in the uniformity of thickness and composition in the growth of compound semiconductors is the temperature uniformity across substrate during growth. The substrate chimney holds the silicon substrate in firm thermal contact with the substrate heater, keeping the temperature uniformity to very close tolerances. The evaporation set-up used in these experiments is a close-coupled system, with source to substrate distance only 5 cm. The evaporation procedure begins at a pressure of about $2 \cdot 10^{-7}$ torr before source heating starts. The pressure rises during the course of the evaporation. Stochiometry of the deposited layer is controlled by changing the composition of the source. For deposition of ternary (pseudo-binary) semiconductors, the source material was a mixture of the binaries. All the films were undoped; the resistivity of the material was very high ($> 10000 \Omega\text{-cm.}$)

On all films, thickness was measured with a Sloan Dektak surface profiler, and the films were analyzed by optical ellipsometry for an additional determination of thickness plus refractive index. Selected films were then subject to further analysis by scanning electron microscopy, x-ray, and EDAX analysis. Typical values of the refractive index were 2.2-2.3. EDAX revealed

that the films were slightly zinc rich.

X-ray diffraction of the films on (100) Si, seen in Figure 3, show many peaks, clearly indicating polycrystalline material. Diffraction from films on (111) Si, shown in figure 4, shows markedly fewer peaks, indicating the deposit is much closer to being an epitaxial crystal. Figure 5 shows a SEM photograph of a thick film grown on (111) Si. The surface is rather rough.

Experiments were made to deposit the ternary compound $ZnS_{(x)}Se_{(1-x)}$ with the composition x chosen at about 0.10 to make the alloy an exact lattice match to Si. Actual composition of the deposited film (as determined by EDAX) was $x=0.04$, indicating that the ZnSe was fractionating from the ZnS during the deposition. The films did not appear to be more crystalline than the ZnS films, and the line of research was not continued further.

Table 2: Standard Evaporation Process Sequence

- (1) Load, argon purge
- (2) High vacuum
- (3) Heater on, 300-375° C degas 1 hr
- (4) Increase to evaporation temp; wait for vacuum to drop to evaporation pressure (typically 25--45 min)
- (5) Bring source up to temperature with shutter closed
- (6) Open shutter, deposit film
- (7) Close shutter; cool-down (typ. 10°C/min)

Analysis Techniques

Two techniques can be used to measure whether the surface recombination velocity has been reduced: first, the open circuit voltage V_{oc} (or alternatively, the dark current I_0) can be measured. Second, the spectral response (or "quantum efficiency," the number of carriers collected per photon absorbed in the cell) in the short wavelength region can be measured. Since short wavelength light is absorbed at shallow depths within the silicon, determining the drop-off of response with decreasing wavelength is a direct and sensitive measure of the surface recombination. Spectral response measurements have the advantage that they are in general

not sensitive to other parameters of the cell such as base diffusion length.

Cell Results

ZnS layers were evaporated on finished solar cells provided by Spire. Electrical characteristics before and after deposition were compared. Three types of cells were used in these experiments:

- (1) Planar (100) Si cells, standard junction
- (2) Planar (100) Si cell, "deep" (0.96 μ) junction [one cell].
- (3) Textured Si cells, lot 4710, "medium" (0.65 μ) junction.

Textured material is (100) silicon that has been etched with an anisotropic etchant to expose (111) planes. The surface after the texture etch consists of tiny pyramids. The orientation of the local surface is very close to the true (111) direction, which differs from (111) Si wafers, which are normally cut a few degrees off-axis.

The deep junction cell was the only one whose photovoltaic performance did not degrade on exposure to temperatures above about 450° C; the ZnS was deposited on this cell at 575° C. Except for one (cell 14-3) in which the ZnS deposition was done at higher temperature (and in which the cell performance was thermally degraded), the ZnS was deposited on the cells at 450° C.

For the planar cells, I-V characteristics were measured with an oxide passivation layer, with the oxide layer removed, and after the ZnS deposition. For the textured cells, the control measurements were made on different cells (11-4 with oxide, 11-5 bare).

Table 3 summarizes the deposition conditions used on these cells. For one of the depositions the prebake (typ. 270° C) was done in hydrogen; for the rest the process was in vacuum.

Table 3: Deposition conditions for cells

Cell #	Vacuum (torr $\times 10^7$)	Substrate temp (°C)	Time (min)	Rate (Å/sec)	Thick (Å)
14-2 (planar)	1.4	452	8	110	810
15-5 (planar)	3.8	575	12	50	580
12-2 (textured)	1.4	452	8	110	875

Table 4 summarizes the electrical measurements of cells with evaporated ZnS. (Electrical measurements tabulated here were performed by Spire Corporation). Some passivation was achieved, as seen in both the short wavelength quantum efficiency and the I_o (or V_{oc}) measurement. The quantum efficiency at 360 nm can be taken as a quick indication of the degree of surface passivation achieved.

Table 4: Cell Electrical Measurements (Best cell of each type)

Surface Orientation	Cell #	Surface Treatment	V_{oc} (mV)	J_o (pA/cm ²)	QE at 360 nm	Diff Length (microns)
(100)	14-2	bare	608	1.0	.058	135
		oxide	631	0.40	.995	134
		ZnS	628	0.51	.257	127
(100)	15-5	bare	611	0.93	.037	124
		oxide	626	0.50	.911	125
		ZnS	621	0.76	.406	120
(111)	11-4	bare	585	3.0	.046	108
	11-1	oxide	596	2.0	.727	105
	12-2	ZnS	601	1.8	.592	101

Figures 6 through 8 show the spectral response measurements (measurements done at Spire Corporation). A short wavelength ("blue") response of ZnS covered cells higher than that of the bare cell indicates surface passivation had occurred. The fact that the response decreases with shorter wavelengths at all indicates that the surface recombination, although lower than that of a bare surface, is not zero. The spectral response of the oxide coated cells can be used as a reference for a nearly-zero recombination surface. (Note that ZnS begins to absorb at wavelengths below 340 nm; this absorption has not been corrected for in the graphs.)

Figure 6 shows the effect of deposition on a planar (100) surface at 450° C. A significant increase in blue response is seen, but not nearly as high a response as the control oxide. Figure 7 shows a deposition on (100) surface at a higher temperature, 575° C. A larger improvement is noted.

Since the deposition was done after cell manufacture, in order to allow

575° C processing a deeper junction cell had to be used.

Figure 8 shows the result on a surface texture-etched to have (111) surface facets. In this cell the short-wavelength response is very close to the oxide control, indicating very low surface recombination velocity.

The diffusion length shown in table 4 is measured from spectral response at long (weakly absorbed) wavelengths. Even on the thermally degraded cells and the cell run at 600° C, the minority carrier diffusion length has not been degraded by the deposition.

CONCLUSIONS

Wide bandgap ZnS heterojunction windows can be formed on silicon and used as minority-carrier mirrors. Demonstration of reduced surface recombination with films at temperatures as low as 450° C is a significant result. For some materials, particularly polycrystalline Si, high-temperature processing such as oxidation results in degradation of the cell; surface passivation by ZnS at low temperatures may be a way to avoid this problem. It also may be significant that the passivation can be done on completed cells.

It is puzzling that the evaporated films, even at temperatures which show passivation on cells, do not appear to be single crystal epitaxial films according to the SEM photos. It is possible that a thin layer at the interface is pseudomorphic epitaxial growth, and that polycrystalline growth nucleates on top of this layer.

Another device where such a layer could be used to advantage is the heterojunction bipolar transistor. By use of a heterojunction emitter to reduce minority carrier injection into the emitter, transistor speed and gain can be increased. The base doping can then be increased, and the base width decreased, resulting in further increases in speed due to the reduced RC charging time, and decreasing deleterious effects such as the Early effect. Although it would be advantageous to produce such heterojunction bipolar transistors on silicon, silicon heterojunction bipolar transistors have not been produced to date because of the absence of a technology for growing a suitable high-bandgap lattice-matched material.

It remains to be demonstrated that these films can be made conductive, and that contacts can be made directly to the ZnS layer, without the need to etch holes to the underlying silicon.

REFERENCES

- [1] M.A. Green *et al.*, *Proc. 19th IEEE Photovoltaic Specialists Conf.*, (1987).
- [2] R.A. Sinton *et al.*, *Proc. 18th IEEE Photovoltaic Specialists Conference*, 39 (1985).
- [3] M.B. Spitzer *et. al.*, *Development of Gallium Phosphide Hereroface Back Surface Field Structures*, Spire Corporation, Final Report for NASA Lewis Research Center Contract NAS3-24642, October 1986; P.A. Sekula *et al.*, *Materials Research Society Meeting*, Anaheim, CA, March 1987.
- [4] R. Hulstrom *et al.*, *Solar Cells* 15, 365 (1985).
- [5] R.J. Anderson, *Solid State Electronics* 5, 241 (1979).
- [6] A.G. Milnes, *Solid State Electronics* 29: 2, 102 (1983).
- [7] L.C. Olsen *et al.*, *Appl. Phys. Lett.*, 34: 8, 528 (1979).
- [8] R.G. Kaufman and P. Dowbor, *J. Appl. Phys.*, 45, 4487 (1974).
- [9] M.P. Godlewski *et al.*, *Proc. 10th IEEE Photovoltaic Specialists Conf.*, 40 (1973).
- [10] D.E. Aspnes, *Surface Science* 132, 413 (1983).
- [11] M.Arienzo and J.J. Loferski, *J. Appl. Phys.*, 51: 6, 3393 (1980).

ACKNOWLEDGEMENTS

This work was carried out under subcontract to Spire Corporation. The work was done in close collaboration with workers from Spire Corporation, without whose help the project could never have been accomplished. In particular we would like to acknowledge the assistance of Mark Spitzer, Stan Vernon, Patricia Sekula, and Chris Keavney.

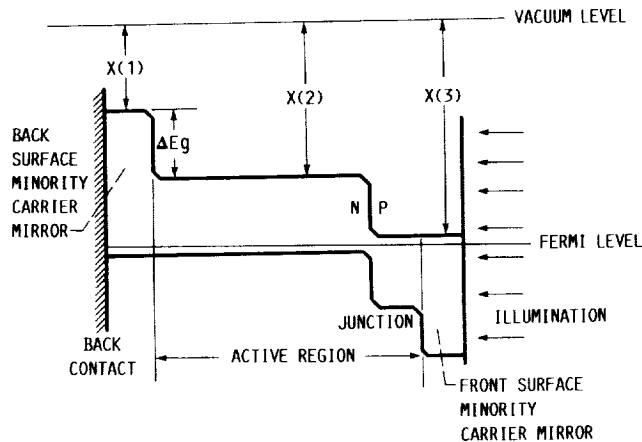


FIGURE 1. - BAND DIAGRAM OF AN IDEAL HETEROJUNCTION MINORITY CARRIER MIRROR.

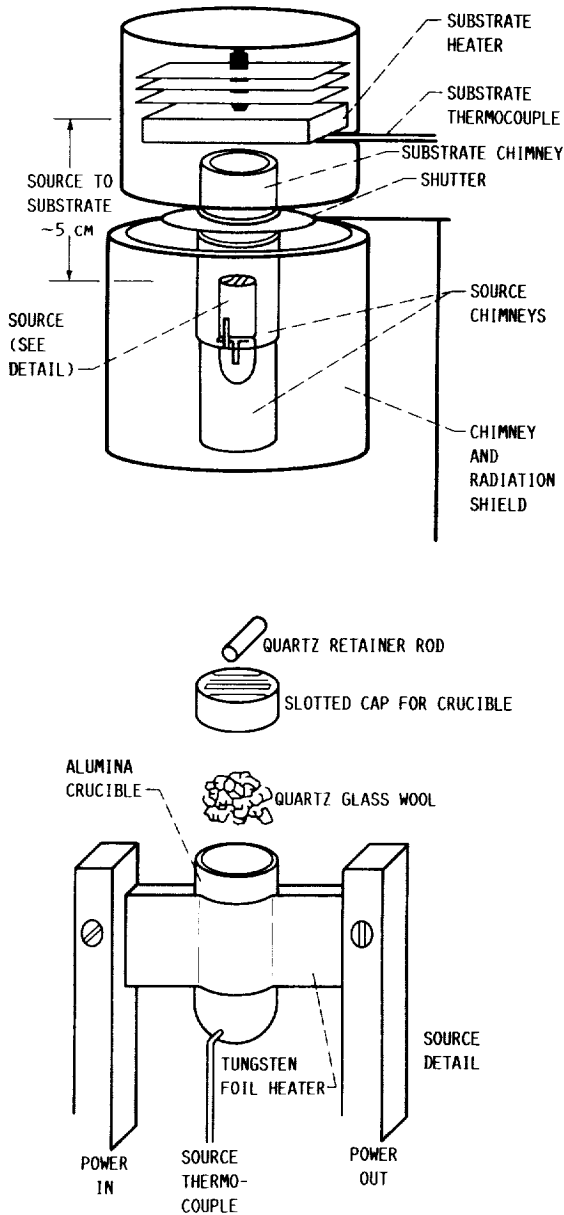


FIGURE 2. - SCHEMATIC OF VACUUM EVAPORATION APPARATUS.

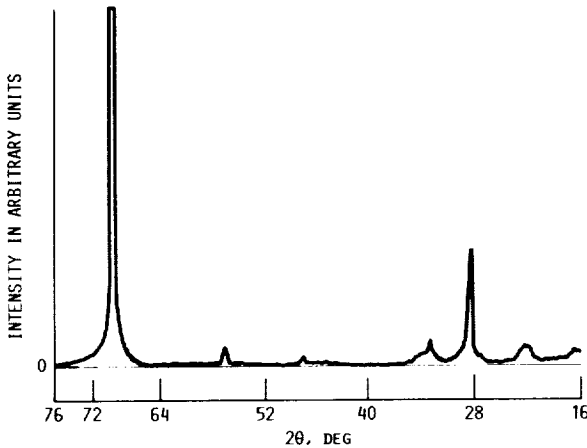


FIGURE 3. - X-RAY DIFFRACTION TRACE OF EVAPORATED ZnS FILM ON (100) Si.

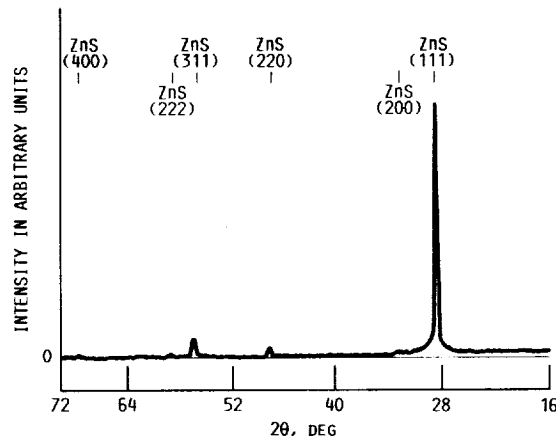


FIGURE 4. - X-RAY DIFFRACTION TRACE OF EVAPORATED ZnS FILM ON (111) Si.

ORIGINAL PAGE IS
OF POOR QUALITY

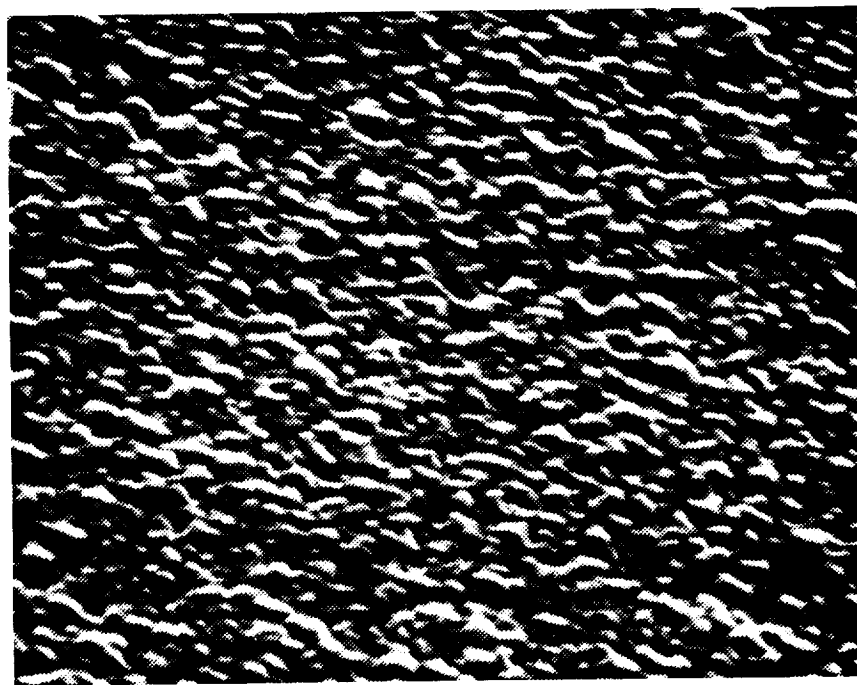
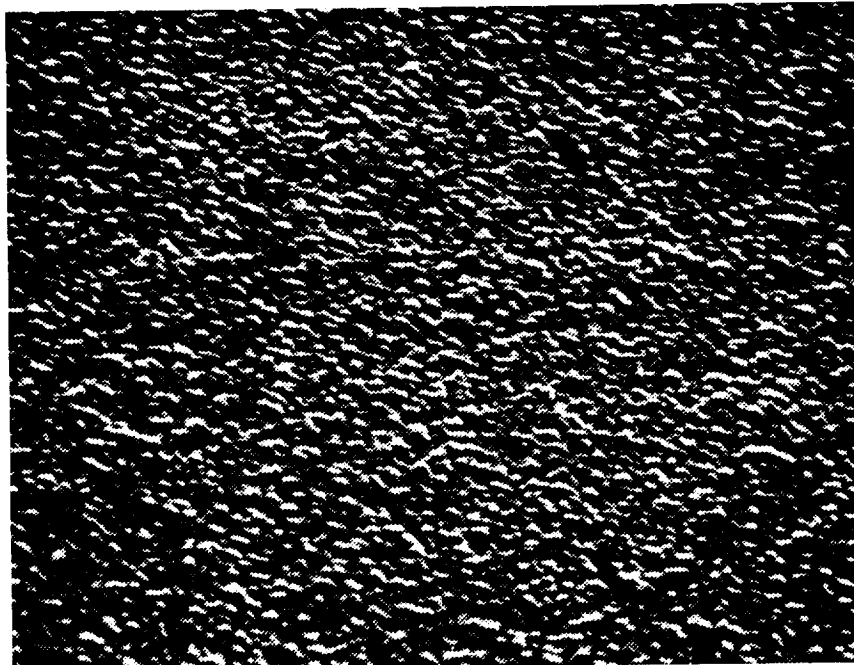


FIGURE 5. - SEM PHOTOGRAPH (45° TILT) OF 8500 Å LAYER OF EVAPORATED ZnS ON (111) Si. TOP:
5000 x. BOTTOM: 9400 x.

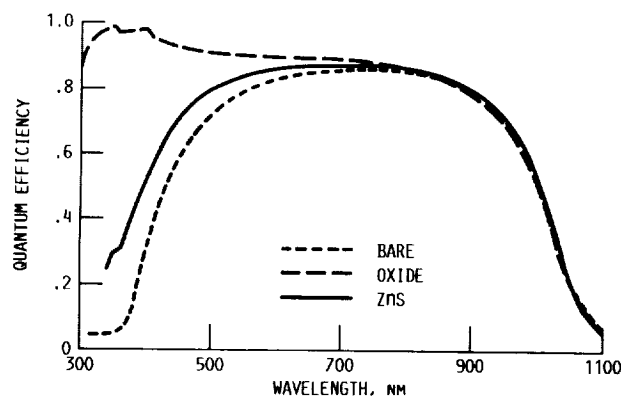


FIGURE 6. - SPECTRAL RESPONSE OF CELL 4660-13-5 (PLANAR SURFACE). (FIGURE COURTESY SPIRE CO.)

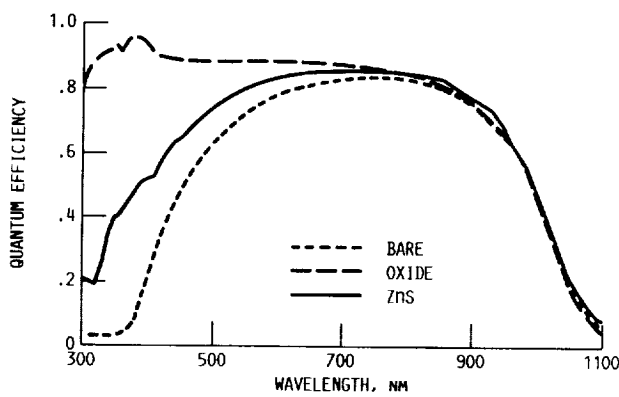


FIGURE 7. - SPECTRAL RESPONSE OF CELL 4660-13-5 (DEEP JUNCTION; ZnS DEPOSITION AT 575 °C). (MEASUREMENT COURTESY SPIRE CO.)

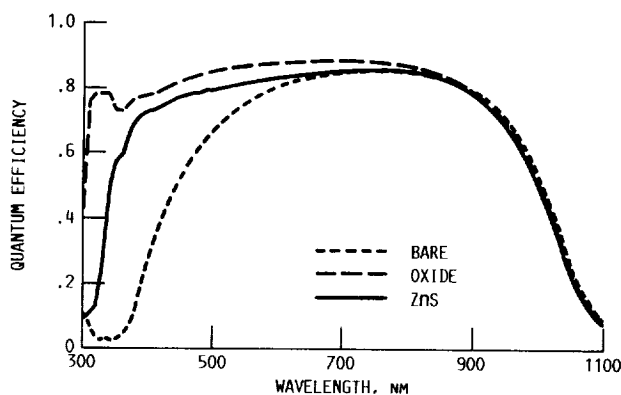


FIGURE 8. - SPECTRAL RESPONSE OF CELL 4710-12-1 (TEXTURED SURFACE). (MEASUREMENT COURTESY SPIRE CO.)



National Aeronautics and
Space Administration

Report Documentation Page

1. Report No. NASA TM-101359	2. Government Accession No.	3. Recipient's Catalog No.	
4. Title and Subtitle Deposition and Characterization of ZnS/Si Heterojunctions Produced by Vacuum Evaporation		5. Report Date	
		6. Performing Organization Code	
7. Author(s) Geoffrey A. Landis, Joseph J. Loferski, and Roland Beaulieu		8. Performing Organization Report No. E-4389	
		10. Work Unit No. 506-41-11	
9. Performing Organization Name and Address National Aeronautics and Space Administration Lewis Research Center Cleveland, Ohio 44135-3191		11. Contract or Grant No.	
		13. Type of Report and Period Covered Technical Memorandum	
12. Sponsoring Agency Name and Address National Aeronautics and Space Administration Washington, D.C. 20546-0001		14. Sponsoring Agency Code	
15. Supplementary Notes Prepared for the Fifth North Coast American Vacuum Society Symposium, Cleveland, Ohio, June 2, 1988. Geoffrey A. Landis, NASA Lewis Research Center; Joseph J. Loferski and Roland Beaulieu, Brown University, Providence, Rhode Island 02912.			
16. Abstract Isotype heterojunctions of ZnS (lattice constant 5.41 Å) were grown on silicon (lattice constant 5.43 Å) p-n junctions to form a minority-carrier mirror. The deposition process was vacuum evaporation from a ZnS powder source onto a heated (450 °C) substrate. Both planar (100) and textured (111) surfaces were used. A reduction of the minority-carrier recombination at the surface was seen from increased short-wavelength quantum response and increased illuminated open-circuit voltage. The minority carrier diffusion length was not degraded by the process.			
17. Key Words (Suggested by Author(s)) ZnS; Epitaxy; Heterojunctions; Heteropitaxy; Solar cells		18. Distribution Statement Unclassified—Unlimited Subject Category 33	
19. Security Classif. (of this report) Unclassified	20. Security Classif. (of this page) Unclassified	21. No of pages 18	22. Price* A03



National Aeronautics and
Space Administration

Lewis Research Center
Cleveland, Ohio 44135

Official Business
Penalty for Private Use \$300

SECOND CLASS MAIL

ADDRESS CORRECTION REQUESTED



Postage and Fees Paid
National Aeronautics and
Space Administration
NASA-451

NASA
